



Original Article

# On the Balance between Magnetization and Coercivity of MnBi Green Powders and Magnets Prepared Thereof

Truong Xuan Nguyen, Ky Hong Vu, Vuong Van Nguyen\*

*Institute of Materials Science, Vietnam Academy of Science and Technology  
18 Hoang Quoc Viet, Cau Giay, Hanoi, Vietnam*

Received 07 February 2020

Revised 21 July 2020; Accepted 15 August 2020

**Abstract:** Currently, MnBi magnetic material is promising to be very potential for low-cost high-temperature permanent magnetic applications. The most attractive parameters are the high magnetocrystalline anisotropy energy and its positive thermal coefficient which allow a high coercivity of MnBi magnets working even at 150 – 200 °C. This advantage is paid by the moderate value of magnetization, so the high energy product of MnBi magnets depends on how one can keep a good balance between the remanent magnetization  $M_r$  and the coercivity  $H_c$ . The paper considers this problem and discusses how to regulate the processing route to keep this balance to enhance the performance of MnBi green powders and MnBi bulk magnets prepared thereof.

*Keywords:* Magnetization, coercivity, balance between magnetization and coercivity, energy product.

## 1. Introduction

Last time, numerous works were done for searching a processing route to prepare high-performance MnBi bulk magnets with the energy product higher the record of 8.4 MGOe reported in [1, 2]. The value of 10 MGOe or more is waited to be reached in short coming time to expand the potential of MnBi magnets in high-temperature magnet applications.

Excluding some magnet applications, for example, in the magnetophysical therapy, the most applications of permanent magnets are based on the magnetic circuits utilizing the maximal energy product  $(BH)_{max}$ . In comparison with the widely used magnets, MnBi magnets own a high and raised-

\*Corresponding author.

*Email address:* [vuongnv@ims.vast.ac.vn](mailto:vuongnv@ims.vast.ac.vn)

<https://doi.org/10.25073/2588-1124/vnumap.4462>

with-temperature coercivity  $iH_c$  which is very attractive feature for high-temperature magnet applications. Unfortunately, the magnetism of MnBi based alloys yields the moderate spontaneous magnetization  $M_s$ . This circumstance causes the balance between remanent magnetization  $M_r$  and coercivity  $bH_c$  to be very important for MnBi magnets in order to improve  $(BH)_{\max}$  of MnBi magnets and make them being a new potential product in the world permanent magnet market.

In this paper we analyze the role of this balance and the technique of regulating it to improve the  $(BH)_{\max}$  of green powders and thus of the bulk magnets prepared thereof.

## 2. Experimental

To produce the MnBi green powders and use them to produce magnets, the alloys with nominal compositions of  $Mn_{50}Bi_{50}$  were arc-melted from the starting high-purity 99.9% metals Mn and Bi under argon atmosphere. The ingots were melted three times to ensure their homogeneity and annealed at 290 °C for 20 h in an argon flow. The green powders were almost fabricated by the Low-Temperature Low-energy Ball-Milling (LTLEBM) route, at which the alloy was by hand crushed and sieved through 400mesh-siever, embedded in pentane and ball-milled at -120 °C. Some times, the high energy ball-milling at the room temperature (RTHEBM) and the low temperature with the liquid nitrogen (LTHEBM) was implemented using the planetary ball-mill machine Pulverisette. All the ball mill were done by 6 mm hard steel balls with the weighing ratio of balls:powders of 10:1. The composition phases of alloys and ball-milling powders were carried out by using D8 advance Bruker X-ray diffractometer (XRD) with  $Cu-K_{\alpha}$  radiation with the scattering angle  $2\theta$  scan in the range from 20 to 80 degrees by the scanning step of  $0.05^\circ$  for 2 s. The phase composition were analyzed by means of Rietveld refinement of XRD patterns for all the obtained diffraction peaks by using the Crystal Impact - Software for Chemists and Material Scientists and, in some cases, by the method of the instant determination of MnBi LTP content presented in the previous work [3]. The morphology of powders was studied by using the Field Emission Scanning Electron Microscopy FESEM Hitachi S-4800. The hysteresis loops of prepared MnBi powders were measured by the Vibration Sample Magnetometer (VSM) with the maximal magnetized magnetic field  $H_{\max}$  of 13.5 kOe.

## 3. Results and Discussion

### 3.1. On the Balance between $M_r$ and $bH_c$

Figure 1 demonstrates magnetization  $M(H)$  and remanence  $B(H)$  loops. For discussion, one uses the loop with very high textured degree of well in-magnetic-field aligned powders or magnets.

The magnet with these  $M(H)$  and  $B(H)$  loops are optimal for hig-energy applications. The load line OL intersects the line closing the points of  $M_r$  and  $bH_c$  at the point P corresponding to the maximal energy product  $(BH)_{\max}$ . The magnet working in this state owns the maximal remanent  $M_r$  which gives raise the high surface magnetic flux required, for example, in the application of permanent magnet generators used in the wind turbines. Moreover, in this state, the remanent coercivity  $bH_c$  is also maximal that means the magnet can work well in a high external magnetic field.

This optimal state requires the following inequality  $bH_c \geq M_r$ , where  $bH_c$  is in kOe, and  $M_r$  – in kG. Correspondingly, the energy product is maximal and calculated by the expression  $(BH)_{\max} = M_r^2/4$ , here  $(BH)_{\max}$  is in MGOe and  $M_r$  – in kG. This gold expression  $bH_c \geq M_r$  must be kept during the route of producing magnets.

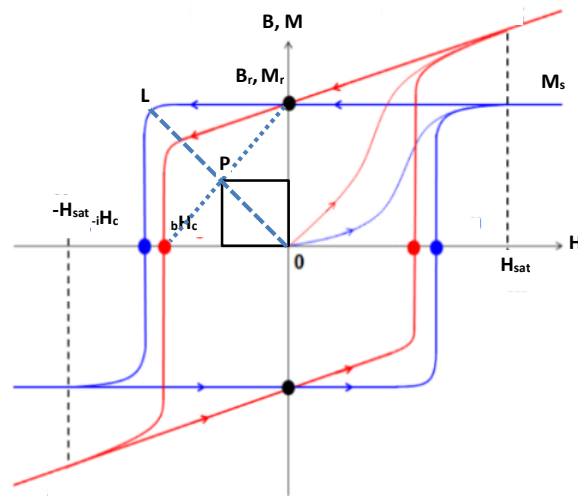


Fig. 1 The typical  $M(H)$  and  $B(H)$  loops of ideally aligned powders or magnets. The loop is balanced by the  $M_r$  vs  $bH_c$  relation when the  $bH_c$  value (in kOe) is equal or greater  $M_r$  value (in kG).

### 3.2. $M_r - bH_c$ Balance of MnBi Magnets

The mentioned gold expression for MnBi bulk magnets requires all the following steps of magnet production route to be well controlled: i) The alloys must be prepared with highest spontaneous magnetization  $M_s$ ; ii) The grinding process must be regulated to keep the  $M_r$  near of  $M_s$ , to increase the coercivity  $iH_c$  (in kOe) larger than  $M_r$  (in kG); iii) To keep the required relation  $bH_c > M_r$  one has to keep  $bH_c$  near  $iH_c$ . Thus the alignment of magnets must be high and must be controlled by using appropriate configurations of the non-magnetic mold, the aligning magnetic field, the manner to keep this alignment during sintering magnets; iv) The use of an optimal compaction pressure  $P_{opt}$  in relation with the size distribution of the powders filled in the mold, this  $P_{opt}$  allow to create dense magnets with the optimal magnetic properties. We discuss these steps below.

#### 3.2.1. The Current Highest Value of $M_s$ of MnBi Alloys

We prepare high- $M_s$  MnBi alloys by using the initial composition of  $Mn_{50}Bi_{50}$ . Numerous works were done with the Mn-enriched initial compositions  $Mn_{50+x}Bi_{50-x}$  [4-6], the obtained results did not show any advantages of this manner in enhancing the content of MnBi ferromagnetic phase (one notes shortly this phase as LTP – Low Temperature Phase since it is formed at temperature lower 340 °C). Fixing the initial composition with the efforts of regulating technological approaches to reach high LTP contents of MnBi alloys one tries to find an appropriate route for producing high-LTP-content MnBi alloys.

The high purity (99.99%) substances of Mn and Bi were weighted in the atomic ratio 1:1 and arc-melted thrice to get high homogeneity. Because of the peritectic solidification of MnBi alloys the LTP content of arc-melted MnBi alloys is below 30 %wt [7]. To increase the LTP content and thus the  $M_s$  value of alloy samples, the arc-melted alloys were subjected to the annealing at around 300 °C for several tens of hours. Once the annealing process is very important, numerous attempts to investigate it [7] to improve its efficiency.

The experimental obtained results show that the most efficient annealing temperature  $T_a$  is 300 °C and the annealing time  $t_a$  is 20 h. At the temperature lower 300 °C the mobility of Bismuth atoms is weaker and drops to zero for 271 °C where the Bismuth is solidified. At the temperature higher 300 °C, although the mobility of Bismuth atoms is high, however, according to the phase diagram [8], the phase formed at this high temperature is preferred to be paramagnetic of  $Mn_{1.08}Bi$ . The saturation annealing time of 20 h is experimental value showing the mechanism of LTP formation during the isothermal annealing process is diffusive as described in Ref. [9] with the mutual diffusion coefficient between Bi and Mn to form LTP phase equal around  $10^{-12} \text{ cm}^2\text{s}^{-1}$ . Because of the peritectic nature of the solidification of MnBi alloys, the random distributions of Bismuth and Manganese clusters inside the arc-melted alloys and the low annealing temperature of the LTphase, the LTP content of annealed alloys stays always around 85-90 %wt. The attempts of applying other methods of annealing, like the multi-time annealing, temperature gradient driven annealing (see for more details in [7]), can increase this content up to 95-98 %wt, and the highest value of  $M_s$  of MnBi alloys is 74 emu/g measured by PPMS equipment at the room temperature RT by 90 kOe magnetic field [10].

### 3.2.2. Variation of $M_s$ and $H_c$ during the Grinding Process

Once again, because of the peritectic solidification of MnBi alloys, the MnBi magnets can't be produced by the casting method even during which the external magnetic field is applied to create the magnetic texture. The bulk MnBi magnets are manufactured using the powder metallurgy method where the alloys are pulverized into green powders that are aligned under external magnetic field in a non-magnetic mold, compacted and sintered into dense bulk magnets.

By using the LTLEBM process, the reduction of grain sizes is demonstrated by the SEM graphs and grain size distributions pictures presented in Fig. 2. The starting powders were by hand crushed and sieved through 400-mesh-siever with the averaged grain size of  $8.5 \pm 3.4 \mu\text{m}$  (Fig. 2a). After 5 min. (Fig. 2b), 120 min. (Fig. 2c) and 180 min. (Fig. 2d) of LTLEBM, the powder assemblies became smooth and the averaged grain sizes are  $5.3 \pm 1.6 \mu\text{m}$ ;  $3.8 \pm 1.6 \mu\text{m}$  and  $3.0 \pm 1.6 \mu\text{m}$ , respectively. It is noted that the longer pulverization can't remarkably reduce the grain sizes.

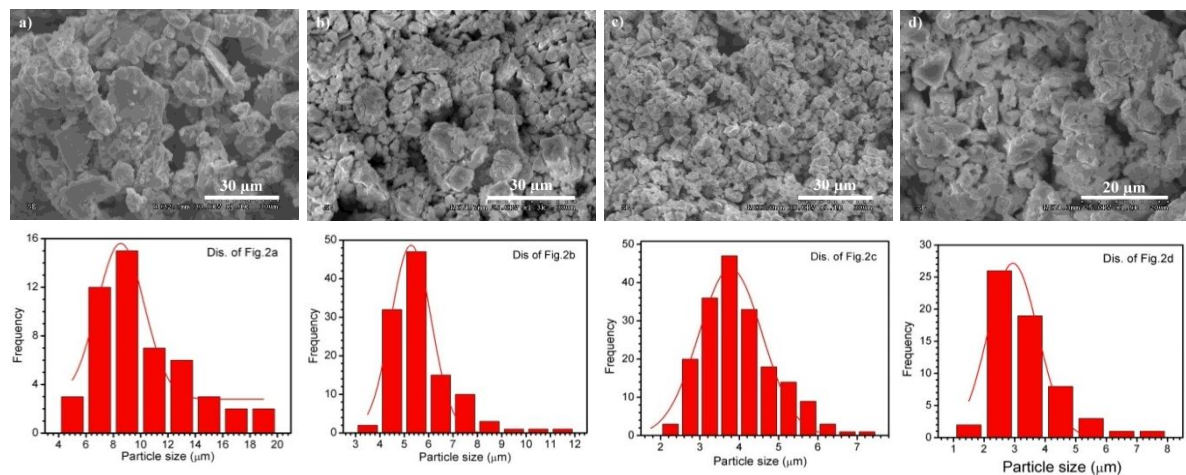


Fig. 2 The variation of grain sizes of MnBi arc-melted and annealed alloy subjected to the in-xylene LTLEBM: The starting sample ground by hand and sieved through 400-mesh-siever (a) and after LTLEBM for 5 min. (b), 120 min. (c) and 180 min. (d).

Normally, the grinding process is assisted with gaining the coercivity until the grain size reaches the domain size limit, the magnetization indeed stays unchanged if the crystal structure is stable under impact forces. However, the MnBi alloys subjected to the grinding process are distinguished by the two inverse variations of  $M_s$  and  $H_c$ : the coercivity is increased by the normal grain size reduction effect but the magnetization is decreased because of the decomposition process of LTP into Bi and Mn. These inverse variations have been observed in all experiments done for fabricating MnBi green powders and stay the noteworthy effect for MnBi material.

To demonstrate this effect, the MnBi in-argon arc-melted and annealed at 300 °C for 20 h alloy was crushed by hand and sieved through 400-mesh-siever into the starting powder and subjected to the in-xylene RTHEBM for different milling times under different impact forces varied by changing the rotating speed. The variations of  $H_c$  and  $M_s$  of powders during this process are shown in Fig. 3. By increasing the milling times,  $H_c$  values of sample are increased, reached saturation or even decreased by decreasing the grain sizes (Fig. 3a). Meanwhile,  $M_s$  values are gradually decreased (Fig. 3b). Under higher impact forces this effect is greater as the results of changes of  $H_c$  and  $M_s$  of powders ground at different rotation speeds of the planetary ball-milling machine.

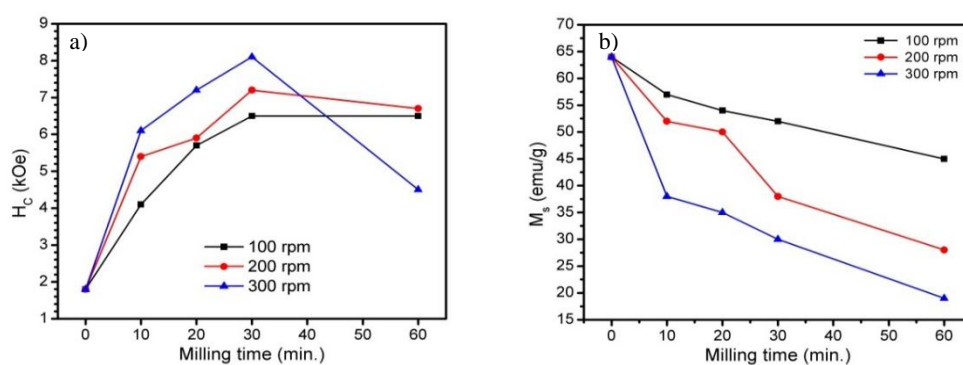


Fig. 3. The variation of  $H_c$  (a) and  $M_s$  (b) of the MnBi arc-melted and annealed alloy subjected to the in-xylene RTHEBM for different milling times and under different rotating speeds of balls.

This abnormal change of  $M_s$  of MnBi powders has been observed in all the experiments done in different laboratories and is believed to be a fundamental effect which seriously affects the current development of MnBi magnets.

To follow more carefully this effect, the MnBi in-argon arc-melted and annealed alloy with highest magnetization  $M_s = 74$  emu/g has been divided into 2-gram batches which were by hand crushed and sieved through 400-mesh-siever into the starting powders and subjected to the in-xylene LTHEBM and LTLEBM for different milling times. The statistical results of the paired values of  $M_s$  -  $H_c$  are plotted in Fig. 4. The starting sample owns  $M_s = 74$  emu/g corresponding to the value of 8.4 kG if the Röntgen mass density  $9.042$  g/cm<sup>3</sup> is taken into account. The coercivity  $H_c$  of this sample is almost around 1 kOe or less. This low value is caused by the big-size particles microstructure.

In order to smooth the grain size in short time, one used LTHEBM. The 15 minutes of this milling is enough to increase  $H_c$  to 7.5 kOe but paid by dropping  $M_s$  to 2.9 kG, this paired value stays far left from the gold triangle discussed below. Instead of the normal way drawn by the dashed line arrow, the variation of paired values of  $H_c$ - $M_s$  of MnBi material follows the direction drawn by the solid line arrow.

Beside the tendency of increasing  $H_c$  paid by decreasing  $M_s$  one also feels a randomness of this variation for different batches of milling even in the case all the batches of 2g of the same starting alloy were used. In Fig. 4, the dotted rectangle covers the  $H_c$ - $M_s$  paired values of samples subjected to

LTLEBM for different milling times. The number appeared near every points are the milling times in minutes. This rectangle area lies under the pattern filled triangle which notes the areas where the above gold expression is satisfied. One calls it as the gold triangle. The results statistically show that, until today, the gold expression can't be easily performed, thus the  ${}_bH_c$ - $M_r$  balance can't be easily realized for any MnBi green powders and bulk magnets, so the energy product  $(BH)_{max}$  stays far below the theoretical upper limit. It is also worthy to note that for the LTLEBM method which is considered as the best tool to fabricate MnBi green powders today, the optimal ball milling time seems around 110 – 120 min. and the obtained  ${}_iH_c$ - $M_s$  paired values lie near below edge of the gold triangle. The further study must be continued to find a novel grinding method to prepare the MnBi powders with  ${}_iH_c$  and  $M_s$  being inside the gold triangle.

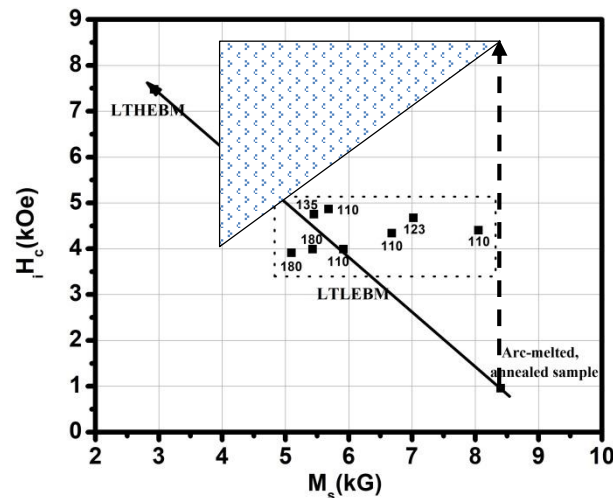


Fig. 4 The variation of  ${}_iH_c$ - $M_s$  paired values of the MnBi arc-melted and annealed alloy subjected to the in-xylene LTLEBM and LTHEBM for different milling times. The numbers written near points are the milling times in minutes.

### 3.2. Alignment of MnBi Green Powders

In order to own the above mentioned gold expression  ${}_bH_c \geq M_r$ , the MnBi green powders are often aligned in a non-magnetic mold by 18kG-magnetic field. The experience shows the best alignment for compacted powders is easily realized in the field perpendicular to the direction of the compaction pressure. The most important to create the alignment is the manner that allows the powder particles freely rotating in the restricted volume of the mold. To keep the alignment of the compacted powders for the final magnet products, the compacted samples must be in-mold sintered. This hot compaction method is very fruitful for manufacturing MnBi bulk magnets, the sintering temperature of which is low around  $\sim 300$  °C.

For comparison of alignment effect, Fig. 5 shows XRD patterns of the powder sample (a), of the parallel surface of the in-epoxy-aligned bonded magnet (b), of the parallel (c) and perpendicular (d) surfaces of the hot compacted and sintered bulk magnet. Almost of peaks belong to the MnBi phase, except small peaks of  $Bi_{(012)}$  at  $27.16^\circ$  and of  $Mn_{(411)}$  at  $43.02^\circ$ . The peak heights of the XRD pattern 3a follow the intensity relation of MnBi phase XRD powder pattern PDF#01-071-4643, this event proves the non-alignment of this powdered sample. In comparison with this, the XRD pattern 3b is featured by peaks of  $MnBi_{(002)}$  and  $MnBi_{(004)}$  which overwhelm all other ones. These two peaks belong to the series



of (001) peaks characterizing the peaks scattered from the basal plane of the unit cell of MnBi. The XRD pattern obtained from the parallel surface of the bulk magnet (pattern 3c) shows also the peak height increase of  $\text{MnBi}_{(002)}$  and  $\text{MnBi}_{(004)}$  and thus the alignment of sintered magnets. The presence of another peaks reveal that the alignment degree of bulk magnet always is far from the ideal alignment caused by the restricted mold volume. In addition, the XRD pattern of the perpendicular surface of bulk magnet (pattern 3d) shows the appearance of  $\text{MnBi}_{(110)}$  and  $\text{MnBi}_{(200)}$  peaks which present the peaks scattered from the side plane. The peak (101) is also observed in this case since it is the strongest peak of MnBi and inclined with the basal plane under angle of  $45^\circ$ .

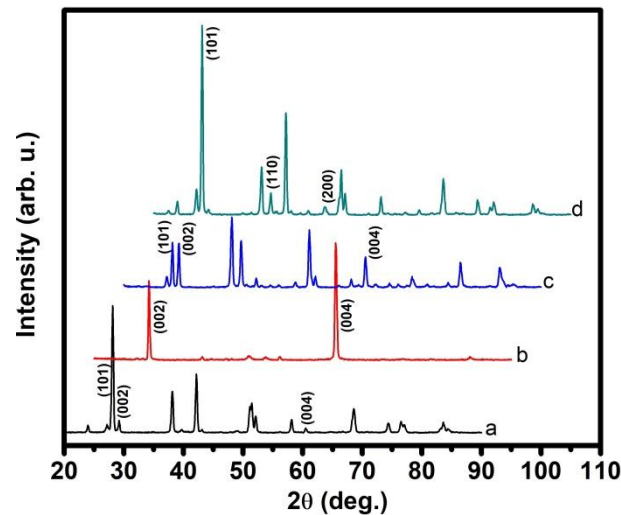


Fig. 5 The XRD patterns taken from: the powdered sample (a), the parallel surface of the in-epoxy aligned magnet (b), the parallel (c) and perpendicular (d) surfaces of the bulk magnet hot-compacted at 2200 psi and measured along the aligning magnetic field. The patterns b, c, d were shifted along  $2\theta$  axis by 5, 10 and 15 deg., respectively, for easy looks.

To characterize the alignment degree  $\zeta$ , one uses the experimental ratio relating the measured intensities between the peak  $\text{MnBi}_{(002)}$  and  $\text{MnBi}_{(101)}$  calibrated to the theoretical value 0.102 of this ratio for the perfect non-alignment case. The coefficient  $\zeta$  is 1 for a non-aligned magnet and infinity for an ideal aligned magnet. For the bonded and bulk magnets shown in Fig. 3,  $\zeta$  is 102 and 10.3, respectively. For the high-performance MnBi bulk magnets with  $(\text{BH})_{\max} = 7.8$  [11] and 8.4 MGOe [1],  $\zeta$  is 15.7 and 45.0, respectively.

The aligned bulk magnet owns the special magnetization loop  $M(H)$  where the magnetization  $M$  is saturated under small measuring field  $H$ , and its remanent magnetization  $M_r$  is closely equal  $M_s$  if the coercivity  $iH_c$  is high enough. In this case, the squareness is also high, and the remanent coercivity  $bH_c$  is also closely to the intrinsic coercivity  $iH_c$ . Totally, if  $M_s$  and  $iH_c$  are inside the area of the gold triangle and the alignment is perfect then the gold expression for  $M_r$  and  $bH_c$  should be easily performed.

#### 3.2.4. Optimization between the Magnet Mass Density and Magnetic Properties

The bulk magnets are final products of magnetic materials. By magnetizing, the magnets catch energy from the external magnetic field and store it in particles included in the volume of compacted and sintered magnets, so the mass density  $\rho$  of magnets plays an important role.

To increase  $\rho$ , a pressure  $P$  is applied and increased gradually to compact the powder assembly filled

inside the mold. The magnetized particles can be considered as mini-magnets, the mutual distance  $r$  between which is resulted by the energy minimization of this mini-magnet system (one calls also the green compaction). Once  $P$  is zero and the space is big enough, the balanced distance  $r_b$  between mini-magnets is determined by minimizing the pushing forces existed between them which are proportional to the magnetized moments  $M$  of particles and  $r^{-4}$ . By increasing  $P$ , the magnet  $\rho$  increases and  $r$  decreases leading to the increment of the green compaction system energy. The in-mold sintering of magnets destroys this energy increment and creates a new state of the system energy minimization which changes the loops of mini-magnets and establishes the final loop of sintered bulk magnets. In fact, this energy minimization can reduce the magnet intrinsic coercivity  $iH_c$  as a result of the change of pushing forces between mini-magnets. In principle, the  $\rho$  enhancement involves the magnet magnetization  $M_s$  as a result of the increasing magnetic moments included in the same space of magnets.

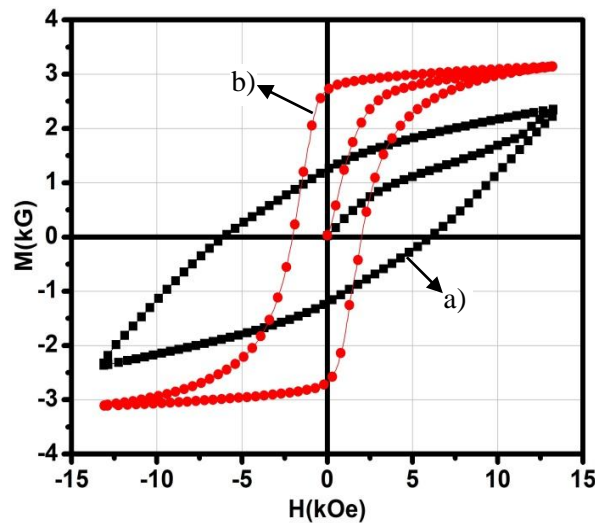


Fig. 6 The loops of the isotropic powder sample (a) and bulk magnet hot-compacted at 2200 psi and measured along the aligning magnetic field (b).

An example of discussed changes of  $M_s$  and  $iH_c$  is shown in Fig. 6. The arc-melted and annealed alloy was LTLEBM for 140 min. into powders. The LTLEBM powder was embedded in an epoxy resin to create an isotropic bonded magnet with  $\rho = 6.8 \text{ g/cm}^3$ . This powder was also used to prepare the bulk magnet using the hot compaction method under 18kG aligning field with the pressure of 2200 psi. One observes that, 140 min. of LTLEBM increased  $iH_c$  from the starting value  $< 1 \text{ kOe}$  up to 5.92 kOe. The value of  $M_s$  measured at 13.5 kOe is 2.36 kG (27.6 emu/g). The remanent magnetization  $M_r$  is 1.26 kG (14.7 emu/g), a half of  $M_s$  as caused by the isotropic nature of the measured sample. After the hot compaction, the magnet became dense with  $\rho = 8.6 \text{ g/cm}^3$ ,  $M_s$  increases to 3.14 kG (29.07 emu/g) because of the mass density increase and  $M_r$  strongly increases to 2.72 kG (25.1 emu/g) since the alignment has been created. Besides, the remarkable feature of these two loops is the big change of  $iH_c$ , from 5.92 kOe of the isotropic bonded magnetle to the lower value of 2.03 kOe of the bulk magnet compacted under pressure of 2200 psi. Moreover, one observes also the change of magnetizing mechanism, from the pinning one of the bonded magnet to the coherent rotation of the hot compacted magnet proved by the shape of their loop initial branches which are bending in the first case and smooth in the other case.

In contrast to the  $iH_c$  vs  $P$  dependence, the  $\rho(P)$  is simply linear for values of  $P$  far from the broken



limit of the mold and pestle. Fig. 7 shows this dependence using six magnets, the green compactions of which were prepared from the same arc-melted and annealed alloy, compacted at different  $P$  and sintered at the same condition of  $300\text{ }^{\circ}\text{C}$  for 10 min. The magnet mass density  $\rho$  (in  $\text{g}/\text{cm}^3$ ) increases by the coefficient  $6.67 \cdot 10^{-4} \text{ gcm}^{-3}/\text{psi}$ .

One understood that, the dependence of magnetic properties, including the energy product  $(\text{BH})_{\text{max}}$ , on the compaction pressure can't be explicitly described since it depends on the particle shape, particle size distribution, the configuration of mold and pestle used. In our case, for MnBi magnets, the experiments shown the optimal compaction pressure  $P_{\text{opt}}$  in the range of  $1600 \div 1800$  psi which create magnets with  $\rho$  of around  $8.5 \text{ g}/\text{cm}^3$  and  $(\text{BH})_{\text{max}}$  of around of  $7.8 - 8.4 \text{ MGOe}$  as

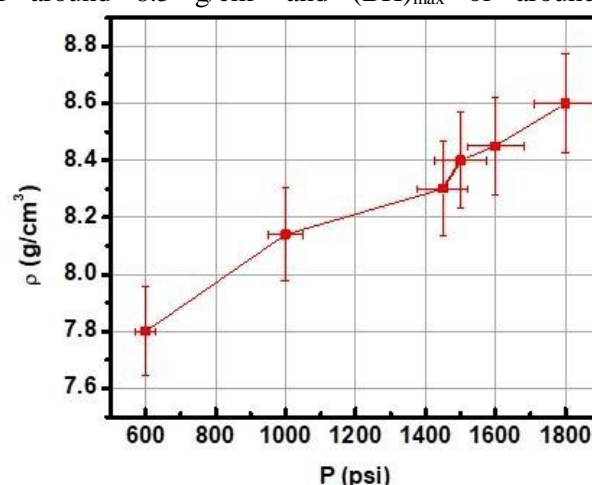


Fig. 7 The dependence of magnet mass density  $\rho$  versus applied compaction pressure  $P$ .

reported in [1, 10].

#### 4. Conclusion

This paper deals with the problem of controlling the balance between the remanent coercivity  $iH_c$  and magnetization  $M_r$  for enhancing the magnet performance. It revealed that the realization of this balance is, in the case of MnBi bulk magnets, crucially required and contributes an important role in enhancing the energy product  $(\text{BH})_{\text{max}}$  of MnBi bulk magnets. It has been proved that to have this balance, the route of producing MnBi bulk magnets should be carefully controlled to i) prepare alloys with the spontaneous magnetization  $M_s$  higher 8 kG; ii) grind alloys into powders owning the relation  $iH_c(\text{in kOe}) > M_r(\text{in kG})$ ; iii) warrantee the high alignment degree  $\zeta$  of the bulk magnet greater 50; iv) use the compaction pressure  $P_{\text{opt}}$  around 1700 psi to reach the magnet mass density  $\rho$  around  $8.5 \text{ g}/\text{cm}^3$ . These listed values are the guide ones for controlling the route of producing high-performance MnBi bulk magnets with  $(\text{BH})_{\text{max}}$  towards the theoretical limit.

#### Acknowledgement

This research is funded by the Vietnam National Foundation for Science and Technology Development (NAFOSTED) under grant number 103.02-2017.327.

## References

- [1] N. Poudyal, X. Liu, W. Wang, V. V. Nguyen, Y. Ma, K. Gandha, K. Elkins, J. P. Liu, K. Sun, M. J. Kramer and J. Cui, Processing of MnBi bulk magnets with enhanced energy product, *AIP Advances* 6 (2016) 056004, <http://doi.org/10.1063/1.4942955>.
- [2] V. V. Nguyen, T. X. Nguyen, Effects of microstructures on the performance of rare-earth-free MnBi magnetic materials and magnets, *Physica B* 532 (2018) 103–107. <https://doi.org/10.1016/j.physb.2017.06.018>.
- [3] T. X. Nguyen and V. V. Nguyen, Preparation and Magnetic Properties of MnBi Alloy and its Hybridization with NdFeB, *Journal of Magnetism* 20(4) (2015) 336-341. <https://doi.org/10.4283/JMAG.2015.20.4.336>.
- [4] J. Cui, J. P. Choi, E. Polikarpov, M. E. Bowden, W. Xie, G. Li, Z. Nie, N. Zarkevich, M. J. Kramer, D. Johnson, Effect of composition and heat treatment on MnBi magnetic materials, *Acta Materialia* 79 (2014) 374–381. <https://doi.org/10.1016/j.actamat.2014.07.034>.
- [5] Y. C. Chen, G. Gregori, A. Leineweber, F. Qu, C. C. Chen, T. Tietze, H. Kronmüller, G. Schüt, E. Goering, Unique high-temperature performance of highly condensed MnBi, *Scripta Materialia* 107 (2015) 131–135. <https://doi.org/10.1016/j.scriptamat.2015.06.003>.
- [6] S. Kim, H. Moon, H. Jung, S. M. Kim, H. S. Lee, H. Choi-Yim, W. Lee, Magnetic properties of large-scaled MnBi bulk magnets, *J. Alloys and Compd.* 708 (2017) 1245 -1249. <https://doi.org/10.1016/j.jallcom.2017.03.067>.
- [7] T. X. Nguyen, V. V. Nguyen, Fabrication of MnBi alloys with high ferromagnetic phase content: effects of heat treatment regimes and dopants, *Journal of Materials Science: Materials in Electronics* 30 (2019) 6888–6894. <http://doi:10.1007/s10854-019-01003-x>.
- [8] K. Oikawa, Y. Mitsui, K. Koyama and K. Anzai, Thermodynamic assessment of the Bi-Mn system, *Materials Transactions* 52 (2011) 2032-2039. <https://doi.org/10.2320/matertrans.M2011229>.
- [9] V. V. Nguyen, T. X. Nguyen, Low temperature phase of the rare-earth-free MnBi magnetic material, *Journal of Science and Technology* 54 (1A) (2016) 50-57. <https://doi.org/10.15625/2525-2518/54/1A/11805>.
- [10] V. V. Nguyen, N. Poudyal, X. Liu, J. P. Liu, K. Sun, M. J. Kramer, and J. Cui, High-performance MnBi alloy prepared using profiled heat treatment, *IEEE Transactions on magnetics*, 50 (2015) 2105506. <http://10.1109/TMAG.2014.2341659>.